Supporting Information

Predicted structures of Agonist and Antagonist Bound Complexes of Adenosine A_3 Receptor

Soo-Kyung Kim,[1] Lindsay Riley,[2] Ravinder Abrol,[1] Kenneth A. Jacobson,[3] and William A. Goddard III[1,*]

[1]Materials and Process Simulation Center (MC139-74),

California Institute of Technology, 1200 E. California Blvd., Pasadena, CA 91125

[2]Department of Biomathematics, University of California, Los Angeles, CA 90095

[3]Molecular Recognition Section, Laboratory of Bioorganic Chemistry, National Institute of Diabetes and Digestive and Kidney Diseases (NIDDK), National Institutes of Health (NIH), Bethesda, MD 20892

Corresponding author:

Prof. William A Goddard III,

Materials and Process Simulation Center (MC139-74),

California Institute of Technology,

1200 E. California Blvd., Pasadena, CA 91125,

Phone: 626-395-2731,

FAX: 626-585-0918,

Email: wag@wag.caltech.edu

- **PredicTM:**

To predict the seven TM domains our current approach (PredicTM) combines hydrophobicity analysis with information from multiple sequence alignments, involving six steps:

i. Retrieval of similar protein sequences from a database (here we select ~2000 sequences with structural identities down to ~ 5%)

ii. Multiple sequence alignment of sequences using the MAFFT[23] multiple sequence alignment program with the "E-INS-i" method, iterative refinement options, in which pairwise alignment information are incorporated into objective function. We find this to be the best suited mode for sequences with multiple aligning segments separated by non-aligning segments, which is the situation for GPCRs. The results for the 4 adenosine receptor subtypes and related sequences are shown in **Fig. 1**.

iii. Hydrophobic profile generation and noise removal. We calculate the consensus hydrophobicity for every residue position in the alignment using the average hydrophobicity of all the amino acids in that position over all of the sequences in the multiple sequence alignment (using the thermodynamic and biological hydrophobic scales from White and von Heijne[24, 25]). Unresolved amino acids in the alignment (B, Z, J, X) are replaced with gaps. Here we eliminate noise by averaging windows of 7 amino acids through 21 amino acids, where 7 corresponds roughly to one helical turn above and below a residue and 21 corresponds roughly to the length of one TMH region. The plot for hAA_3R is shown in **Fig. S1** of Supporting Information.

iv. Initial TMH region predictions. The initial TMH domain predictions are simply the regions with hydrophobicity values greater than zero, resulting in "raw helices."

v. Application of capping rules. The raw helices are extended (or capped) on both N- and C-termini until a “helix breaker” residue is found. To predict correctly this secondary structure outside the membrane, we extend both sides of the predicted hydrophobic regions using consensus helices based on the APSSP2[26] and PORTER[27] servers.

vi. Identification of hydrophobic centers: To place all helices on the same reference plane we select the “hydrophobic center” for each helix as the position in the raw helix where the geometry hydrophobic center is equal on both sides. The results of these last 3 steps are shown in **Table S1** of Supporting Information.

Table S1. The predicted seven transmembranic helix (TMH) regions and hydrophobic centers (HPC). The raw helices are extended (or capped) on both N- and C- termini until a "helix breaker" residue is found. To predict correctly this secondary structure outside the membrane, we extend TM3 and 6 using consensus helices based on the secondary structure prediction, APSSP2[26] and PORTER[27] servers.

TMH		Start	Sequence	Stop	Length	HPC
1	Raw	13	VTYITMEIFIGLCAIVGNVLVICVV	37	25	25.5
	Cap	9	SLANVTYITMEIFIGLCAIVGNVLVICVVK	38	30	24.0
2	Raw	47	TFYFIVSLALADIAVGVLVMPLAIVVS	73	27	60.5
	Cap	47	TFYFIVSLALADIAVGVLVMPLAIVVS	73	27	60.5
3	raw	81	YSCLFMTCLLLIFTHASIMSLLA	103	23	92.5
	cap	81	YSCLFMTCLLLIFTHASIMSLLA	103	23	92.5
	SS	81	YSCLFMTCLLLIFTHASIMSLLAIAVDRYLRVK	113	33	97.5
4	raw	129	LALGLCWLVSFLVGLTPMF	147	19	138.5
	cap	126	RIWLALGLCWLVSFLVGLTPMFG	148	23	137.5
5	raw	177	MVYFSFLTWIFIPLVVMCAIYLDI	200	24	189.0
	cap	175	DYMVYFSFLTWIFIPLVVMCAIYLDIFYIIR	205	31	190.5
6	raw	233	FLVLFLFALSWLPLSIINCII	253	21	243.5
	cap	230	KSLFLVLFLFALSWLPLSIINCII	253	24	242.0
	SS	219	GAFYGREFKTAKSLFLVLFLFALSWLPLSIINCII	253	35	236.5
7	raw	265	YMGILLSHANSMMNPIVY	282	18	274.0
	cap	265	YMGILLSHANSMMNPIVYAYK	285	21	275.5

- HPC: PredicTM raw geometric hydrophobic center

- cap: capped helix extension

- SS: helix extension from the secondary structure prediction

Table S2. Top 7 ligand conformations of Cl-IB-MECA ordered by mpsim total energy (TotE, kcal/mol) from Conformational search. The torsion angles C_{ar}-C_{ar}-NH-C_{al} (Tot1) and C_{ar}-NH-C_{al}-C_{ar} (Tot2) between the adenine ring and the benzyl substituent were rotated by 60 ° increments to generate 36 conformations. We selected the lowest 7 ligand conformations in grey shading (within 3 kcal/mol of the best E) for docking. The final docked structure with the best binding E is shown in bold face.

#	Tot1	Tot2	TotE
28	-176.18	-179.45	46.05
16	173.67	167.24	46.98
24	179.27	-71.28	48.54
23	-179.75	-120.64	48.61
21	**-178.25**	**118.41**	**48.80**
8	27.11	86.64	49.19
11	33.21	-107.98	49.22
7	7.05	63.21	49.25
22	-179.02	178.75	49.34
10	17.77	-163.16	49.38
27	-138.51	119.65	49.60
13	156.50	-70.48	49.60
4	-2.49	-176.77	49.87
19	166.01	-9.84	50.25
9	36.92	131.94	50.31
3	-5.19	117.21	50.36
2	1.13	65.23	50.51
5	1.66	-111.64	50.57
20	-175.38	65.27	51.07
6	-6.04	-59.74	51.30
30	-144.33	-58.59	51.57
29	-135.58	-116.71	51.81
26	-138.88	75.54	52.05
15	137.01	115.85	52.07
18	139.81	-80.69	52.20
17	132.36	-123.60	52.55
34	-34.86	173.21	52.88
33	-47.91	114.61	53.43
25	-152.12	66.02	53.60
31	-14.38	-56.87	53.84

35	-49.86	-123.49	53.87
36	-40.95	-74.57	54.34
12	49.29	-64.68	54.59
1	32.47	1.91	55.44
14	137.88	59.55	56.52
32	-67.11	72.99	56.65

Table S3. The relative difference of the six degrees of freedom for each helix (x, y, z, θ, φ, η) among the x-ray structures of turkey β_1 adrenergic (PDB ID: 2vt4) and human adenosine A_{2A} receptors (PDB ID: 3eml) compared to human β_2 adrenergic receptor (PDB ID: 2rh1).

Turkey β1 adrenergic receptor									
TM	EtaRes		δX	δY	δHPC	δTheta	δPhi	δEta	δSTD
1	N	59	-0.55	-0.56	0.29	2.70	-3.54	3.41	2.52
2	D	87	-0.22	0.00	-0.01	1.75	2.56	-6.01	3.01
3	D	121	0.00	0.00	0.06	0.20	0.94	-1.74	0.88
4	W	166	0.02	0.07	-0.14	-0.81	4.22	4.92	2.50
5	P	219	-0.04	0.11	-0.23	0.05	4.34	-0.52	1.84
6	P	305	-0.31	-0.03	-0.07	0.20	-6.14	-3.84	2.66
7	P	340	-0.20	-0.14	0.17	-3.36	-0.55	3.35	2.14
		STD	0.20	0.23	0.18	1.93	3.96	4.11	1.77
Human adenosine A2A receptor									
TM	EtaRes		δX	δY	δHPC	δTheta	δPhi	δEta	δSTD
1	N	24	1.90	1.80	-0.15	5.79	16.88	3.99	6.15
2	D	52	0.20	0.00	0.17	7.26	2.16	-19.58	9.22
3	V	84	0.00	0.00	0.20	4.88	2.30	-14.15	6.66
4	W	129	-1.28	-0.19	0.24	-4.50	-5.21	-9.95	3.88
5	P	189	0.07	-0.51	0.79	-0.90	15.29	-0.89	6.39
6	P	248	0.70	0.16	0.49	10.59	-36.17	0.05	16.27
7	P	285	-0.08	1.15	0.26	3.95	-0.01	1.83	1.55
STD			0.95	0.82	0.29	5.07	17.61	9.03	5.63

- STD: standard deviation

Table S4. The relative difference of the six degrees of freedom for each helix (x, y, z, θ, φ, η) of the x-ray structures of opsin (PDB ID: 3cap) compared to bovine rhodopsin (PDB ID: 1u19).

TM	EtaRes		δX	δY	δHPC	δTheta	δPhi	δEta	δSTD
1	N	55	-0.55	-0.18	0.37	2.24	-4.64	-3.35	2.53
2	D	83	0.08	0.00	-0.20	-2.12	-1.87	8.73	4.02
3	A	117	0.00	0.00	-0.49	-0.63	-9.43	-26.02	10.43
4	W	161	1.50	1.06	0.50	-1.03	-9.62	-14.42	6.70
5	P	215	-1.18	3.25	0.16	0.10	-21.94	-4.54	9.13
6	P	267	0.44	3.43	-0.02	3.61	39.84	-28.57	21.77
7	P	303	-0.01	0.75	0.09	3.01	-11.19	0.24	5.03
		STD	0.83	1.54	0.34	2.21	19.79	13.85	6.42

- STD: standard deviation

Table S5. Top 10 predicted structures of human adenosine A_1 and A_{2B} receptors from the CombiHelix analysis of the $(7)^7$ = 823,000 BiHelix packing geometries within ± 45 ° angle range by 15 ° increments. All 1,000 predicted structures from CombiHelix were selected for neutralization by their charge total energy score (ChargeTot: kcal/mol). The final 100 predicted structures are ordered by neutral total energy (NeutTot: kcal/mol). The case with η = 0 ° for all 7 helices (same as in the experimental antagonist bound $A_{2A}R$ structure) is shown in grey shading.

			A_1								
H1	**H2**	**H3**	**H4**	**H5**	**H6**	**H7**	**ChargeIH**	**ChargeTot**	**NeutIH**	**NeuTot**	**W6.48 χ1**
0	0	0	0	0	0	0	-360.2	465.1	-325.4	327.5	-67.8
0	0	0	15	0	0	0	-340.5	467.0	-319.9	329.7	-67.8
0	0	15	0	0	0	0	-361.5	445.4	-330.8	335.6	-67.6
0	0	15	-30	0	0	0	-365.9	428.5	-320.6	340.0	-67.3
0	0	15	-15	0	0	0	-350.5	457.3	-321.2	351.6	-67.6
0	0	0	0	15	45	15	-313.4	508.2	-296.5	355.4	171.6
0	0	0	0	15	15	0	-320.2	500.5	-301.9	359.2	153.5
0	0	0	0	-15	0	0	-378.1	496.4	-331.4	359.8	-67.5
0	0	15	15	0	0	0	-335.1	465.3	-317.8	360.6	-67.7
0	0	15	0	0	15	0	-341.8	486.3	-319.0	363.6	-175.0
			A_{2B}								
H1	**H2**	**H3**	**H4**	**H5**	**H6**	**H7**	**ChargeIH**	**ChargeTot**	**NeutIH**	**NeuTot**	**W6.48 χ1**
0	0	0	0	0	0	0	-410.4	78.6	-372.2	-24.2	-78.9
0	0	0	15	0	0	0	-384.5	99.0	-360.5	-5.3	-79.0
0	0	0	0	15	0	0	-390.1	128.0	-360.2	-4.3	-78.9
0	0	0	15	15	0	0	-360.5	142.7	-343.1	7.5	-79.0
0	0	0	0	15	15	0	-391.3	128.4	-358.6	11.0	-144.8
-15	0	0	0	0	0	0	-402.7	111.7	-357.6	14.3	-78.9
0	0	0	0	-15	0	0	-392.7	153.3	-373.0	14.8	-79.1
0	0	0	15	15	15	0	-359.0	138.8	-335.3	18.2	-144.8
0	0	0	15	-15	0	0	-382.3	143.6	-367.6	18.5	-79.1
-15	0	0	0	15	0	0	-388.7	142.6	-349.2	23.9	-78.9

- ChargeIH (Charge interhelical energy), ChargeTot (Charge total energy), NeutIH (Neutral interhelical energy), NeutTot (Neutral total energy)

Table S6. Analysis of dominant interactions among the 20 most stable predicted structures of human A_3 adenosine receptor (from the SuperBiHelix/ CombiHelix analysis in Table 2). The predicted structures are ordered by neutral total energy (NeutTot: kcal/mol).

	Hetero-atom distance in the salt-bridge					**Hetero-atom distance in the Hbond**		
#	**D107$^{3.49}$: R111$^{3.53}$**	**D107$^{3.49}$: R126$^{4.41}$**	**R108$^{3.50}$: E225$^{6.30}$**	**E225$^{6.30}$: R224$^{6.29}$**	**K113$^{3.55}$: D199$^{5.60}$**	**N30$^{1.50}$: N278$^{7.49}$**	**D58$^{2.50}$: N278$^{7.49}$**	**Y109$^{3.51}$: K113$^{3.55}$**
1	4.2	6.7	8.1	3.5	2.3	2.9	2.7	2.8
2	3.7	5.4	7.9	3.2	2.5	2.9	2.7	2.8
3	11.2	4.1	7.9	3.4	3.2	2.9	2.7	2.7
4	3.7	5.4	8.5	3.2	2.5	2.7	4.0	2.8
5	3.7	5.4	7.9	3.4	3.1	2.9	2.7	3.0
6	3.8	6.3	8.2	3.2	4.4	3.8	4.9	3.1
7	4.1	7.1	7.9	3.4	3.1	2.9	2.7	3.0
8	10.1	6.7	5.7	4.7	2.5	4.8	2.8	2.8
9	3.7	5.4	7.9	3.2	2.5	2.9	3.2	2.8
10	4.2	7.3	7.9	3.4	3.1	2.9	2.7	3.0
11	3.7	5.4	8.2	3.2	4.0	2.9	2.7	3.2
12	9.6	4.6	5.7	4.7	2.5	4.8	2.8	2.8
13	11.8	4.4	14.2	3.4	3.1	2.7	4.0	2.9
14	3.7	5.4	7.9	3.4	5.2	2.9	2.7	3.5
15	3.8	4.5	7.9	3.2	2.3	4.6	4.9	2.8
16	3.7	5.4	4.9	5.0	3.4	5.4	3.1	2.8
17	4.2	7.3	7.9	3.4	3.1	2.7	4.0	2.9
18	4.2	7.3	7.9	3.4	3.1	3.0	4.5	2.9
19	11.9	3.3	7.9	3.4	3.2	2.9	2.7	2.7
20	3.7	5.4	8.0	3.4	4.5	5.4	3.9	2.8

Table S7. The χ_1 angle of three toggle switch residues, W243$^{6.48}$, Y282$^{7.53}$, and R108$^{3.50}$, of top 20 predicted structures of human A_3 adenosine receptor (from the SuperBiHelix/ CombiHelix analysis). All A_3 agonists stabilize the 15th lowest conformation in orange shade, while the A_3 antagonists stabilize the 2nd lowest conformation in yellow shade.

#	Torsion χ1 (apo-protein)			Torsion χ1 (Agonist)			Torsion χ1 (Antagonist)		
	W243	**Y282**	**R108**	**W243**	**Y282**	**R108**	**W243**	**Y282**	**R108**
1	-85.5	-64.9	-73.6	-174.9	-66.1	-73.4	-80.3	-66.0	-73.2
2	-75.8	-65.0	-73.4	-164.5	-68.5	-71.8	-80.2	-68.5	-71.8
3	-85.3	-57.7	-167.7	-70.9	-56.8	-173.9	-79.2	-56.8	-173.9
4	-75.6	-72.3	-73.5	-174.9	-75.0	-72.7	-80.3	-74.9	-72.8
5	-85.3	-51.4	-167.5	-69.4	-51.5	-172.8	-80.1	-51.5	-172.7
6	-85.4	-173.9	-73.7	-170.9	-174.1	-75.2	-79.6	-174.1	-75.2
7	-85.4	-65.0	-167.6	-70.9	-66.4	-172.2	-79.0	-66.5	-172.1
8	-85.4	-64.7	-73.6	-164.0	-67.3	-71.6	-79.2	-67.3	-71.9
9	-75.6	-71.1	-73.4	154.7	-72.6	-71.6	-84.8	-72.6	-71.6
10	-85.5	-64.9	-167.6	-70.6	-66.5	-172.6	-79.1	-66.5	-172.6
11	-85.2	-65.0	-73.9	-171.2	-68.4	-75.0	-80.8	-68.4	-75.0
12	-85.3	-64.7	-73.6	-163.8	-67.4	-70.8	-79.5	-67.4	-70.8
13	-85.6	-72.3	-67.7	-69.5	-75.1	-70.6	-80.9	-75.0	-70.6
14	-85.3	-59.9	-167.5	-165.8	-60.0	-172.9	-80.2	-59.9	-173.0
15	-75.8	-67.9	-73.4	154.4	-64.2	-73.2	-80.1	-64.2	-73.2
16	-85.5	-60.8	-169.4	-171.0	-63.2	-169.4	-79.3	-63.3	-169.4
17	-85.6	-72.2	-167.6	-69.2	-75.1	-172.5	-81.2	-75.1	-172.6
18	-75.6	-79.8	-167.6	-69.4	-81.2	-172.6	-95.8	-81.2	-172.7
19	-85.3	-60.6	-167.8	-69.3	-61.2	-173.3	-80.1	-61.1	-173.3
20	-75.5	-51.4	-74.0	-171.3	-53.9	-75.8	-95.6	-53.9	-75.9

Table S8. DarwinDock results for the final top 25 poses for adenosine bound to lowest predicted structure of adenosine A_3 receptor (AA_3R). Predicted structures are ordered by the average ranking (Avg Rnk) of total (Tot) and unified cavity (Ucav) energies (kcal/mol). The lowest energy from each energy scoring is underlined. The predicted most stable adenosine/ AA_3R complex based on unified cavity energy is underlined.

Cluster #	Avg Rnk	Tot	UCav
c1276	3.5	-903.76	-36.64
c17285	6.0	-892.47	-33.48
c6058	6.0	-889.82	-38.43
c17748	6.5	-900.41	-30.29
c17395	7.0	-892.24	-32.00
c24528	7.0	-905.33	-28.38
c350	8.5	-893.19	-29.65
c34565	9.0	-874.32	-35.20
c16055	11.5	-891.79	-26.72
c513	13.5	-905.24	-18.49
c38371	13.5	-883.52	-26.69
c3362	13.5	-870.15	-29.74
c9913	13.5	-906.19	-1.77
c37036	14.0	-888.92	-25.59
c37853	14.5	-904.49	-12.42
c16239	14.5	-859.81	-31.81
c30401	15.5	-874.49	-24.71
c18478	16.5	-857.07	-29.66
c5512	17.5	-871.10	-24.59
c32005	18.0	-873.90	-23.85
c23634	18.5	-831.86	-29.51
c31371	20.0	-849.71	-26.34
c13623	20.0	-870.92	-21.55
c12475	20.5	-862.89	-24.03
c4971	21.0	-864.81	-23.85

- Tot: total energy of the neutral complex, UCav: non-bonding cavity E of unified cavity

Table S9. DarwinDock results for the total 125 poses for Cl-IB-MECA. Total 125 poses from 25 poses of five different ligand conformations are re-ordered by the average ranking (Avg Rnk) of total (Tot) and unified cavity (Ucav) energies (kcal/mol). The conformation number is from the energy order of the conformational search. The predicted most stable complex based on unified cavity energy is underlined.

Conf #	Cluster #	Avg Rnk	Tot	UCav
4	c2202	2.5	-534.82	-44.94
2	c18650	10.5	-531.52	-41.01
4	c420	11.5	-526.01	-43.26
4	c12301	13.5	-533.55	-39.80
4	c17790	15.5	-519.37	-44.40
4	c8959	15.5	-532.12	-39.17
2	c17930	17.5	-516.05	-50.33
4	c7005	19.0	-519.33	-42.01
3	c11193	20.5	-514.72	-44.84
4	c4734	21.0	-530.98	-38.47
4	c217	21.0	-540.71	-37.82
3	c12951	21.5	-530.13	-38.55
4	c13791	22.5	-514.54	-44.66
2	c5829	26.0	-513.95	-42.74
3	c935	26.0	-520.50	-39.00
4	c10278	28.0	-517.64	-39.20
4	c19180	28.0	-531.03	-36.88
2	c5220	29.0	-525.70	-37.99
4	c16175	29.5	-514.03	-40.65
4	c12851	29.5	-525.80	-37.73
4	c10462	31.0	-512.93	-40.48
2	c14688	31.0	-530.78	-36.24
4	c2927	31.5	-509.64	-42.89
2	c16706	32.5	-511.11	-41.01
4	c350	35.5	-515.39	-38.31
2	c5760	36.5	-510.35	-39.95
1	c1431	37.0	-508.04	-42.46
2	c3889	37.0	-508.55	-41.37
4	c1906	37.5	-525.33	-35.97
4	c10605	39.0	-527.00	-35.38
2	c3297	40.5	-508.46	-40.06
1	c14552	41.5	-529.60	-34.04

4	c9525	42.0	-511.31	-38.11
4	c13377	42.0	-522.48	-35.49
1	c11696	42.5	-506.61	-40.74
5	c5835	43.0	-509.58	-38.89
2	c8325	44.5	-507.33	-39.57
2	c2122	45.0	-522.26	-34.59
1	c16495	45.5	-511.14	-37.70
2	c1139	46.5	-526.26	-33.45
4	c12995	48.0	-508.57	-38.22
2	c13438	49.0	-515.01	-35.51
4	c17812	49.0	-516.98	-35.30
4	c15333	50.0	-514.63	-35.53
3	c3208	51.5	-508.85	-37.18
5	c8685	53.5	-501.59	-39.98
5	c6114	53.5	-505.29	-38.36
1	c12072	54.5	-508.40	-37.18
2	c17328	56.5	-491.66	-43.15
3	c11882	57.5	-508.62	-35.97
2	c12559	58.5	-520.35	-31.12
5	c8874	59.0	-506.87	-36.28
4	c1722	59.5	-542.29	-22.91
1	c12464	62.0	-518.53	-30.54
2	c4389	62.5	-510.22	-33.84
1	c8984	63.0	-518.19	-30.20
4	c19512	63.0	-526.11	-26.25
1	c10102	63.5	-503.23	-36.99
1	c8087	64.0	-515.57	-30.78
5	c19231	64.5	-482.81	-41.75
3	c320	64.5	-493.10	-39.05
1	c4647	64.5	-534.71	21.31
2	c16815	65.5	-509.57	-33.69
1	c18300	66.5	-492.14	-38.97
1	c13348	67.5	-511.76	-31.72
1	c18303	67.5	-527.68	-17.14
1	c3142	68.0	-496.43	-37.70
2	c6395	69.5	-488.05	-39.06
3	c2304	69.5	-512.15	-30.71
3	c4875	70.5	-524.64	-22.21
5	c12150	73.5	-504.85	-33.77
3	c13231	74.0	-503.25	-34.24
3	c16803	74.0	-506.28	-33.46
1	c18389	74.0	-517.88	-23.05
5	c17222	74.5	-494.38	-36.56

3	c10693	76.0	-481.18	-38.60
1	c5497	76.5	-485.68	-38.07
1	c18795	76.5	-503.38	-33.66
3	c5519	77.0	-491.90	-36.64
3	c5448	77.0	-517.96	3.88
1	c16262	78.0	-492.43	-36.22
2	c9500	78.0	-511.05	-27.65
5	c14944	78.5	-504.47	-32.94
1	c17888	79.0	-506.47	-31.76
3	c10631	79.5	-494.37	-35.61
1	c3940	80.0	-511.20	-25.56
2	c3412	80.0	-514.65	-21.71
2	c11833	80.5	-502.14	-33.34
5	c15767	80.5	-504.42	-32.5
5	c4877	81.5	-490.27	-36.15
5	c1711	82.5	-491.58	-35.71
5	c7813	84.0	-474.01	-37.43
1	c9434	84.0	-509.81	-24.99
3	c13553	84.5	-488.59	-35.76
1	c19787	84.5	-506.77	-29.41
5	c1782	85.0	-501.74	-32.51
5	c4439	86.5	-494.51	-33.56
3	c2145	86.5	-499.22	-32.69
1	c1295	87.5	-494.95	-33.25
3	c9183	89.0	-505.31	-27.49
2	c17292	89.0	-507.95	-25.14
5	c9381	89.5	-499.38	-31.61
2	c7578	90.0	-502.71	-29.69
5	c11766	90.5	-482.58	-35.47
2	c4709	91.0	-493.58	-33.14
5	c10280	91.0	-494.77	-32.26
5	c5009	92.5	-481.94	-35.1
2	c7547	92.5	-494.50	-32.11
1	c12102	92.5	-502.08	-29.26
3	c4521	93.0	-499.01	-30.57
5	c9278	95.0	-480.14	-34.51
5	c11301	96.5	-504.18	-23.41
5	c3087	97.5	-467.51	-34.09
3	c229	98.5	-496.43	-28.70
3	c16808	99.5	-496.82	-27.08
3	c17230	101.5	-500.99	-24.98
3	c6702	102.0	-501.80	-22.74
3	c5069	103.5	-501.99	-0.20

1	c12935	104.0	-488.87	-29.76
5	c8641	105.5	-488.6	-29.66
5	c17960	107.0	-477.62	-31.2
3	c14787	108.5	-491.32	-26.45
3	c3496	110.0	-485.23	-28.07
5	c13431	112.5	-485.99	-25.59
5	c2005	114.0	-481.66	-26.52

- Tot: total energy of the neutral complex, UCav: non-bonding cavity E of unified cavity

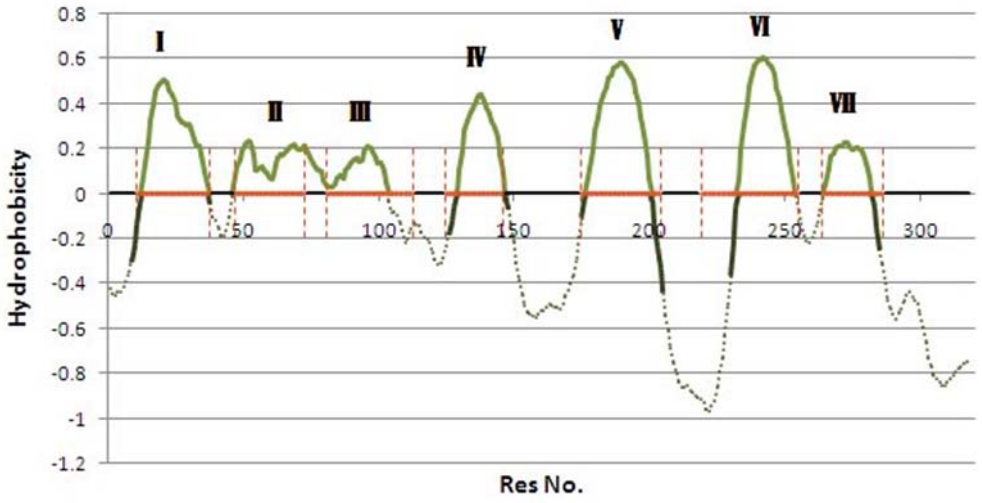

Figure S1. The hydropathy prediction from GEnSeMBLE method for human adenosine A_3 receptor at window size 7 to 21. Initial transmembrane (TM) raw and capped helixes are shown with green and black line, respectively. The 7 TM regions from the homology helix are displayed in red line.

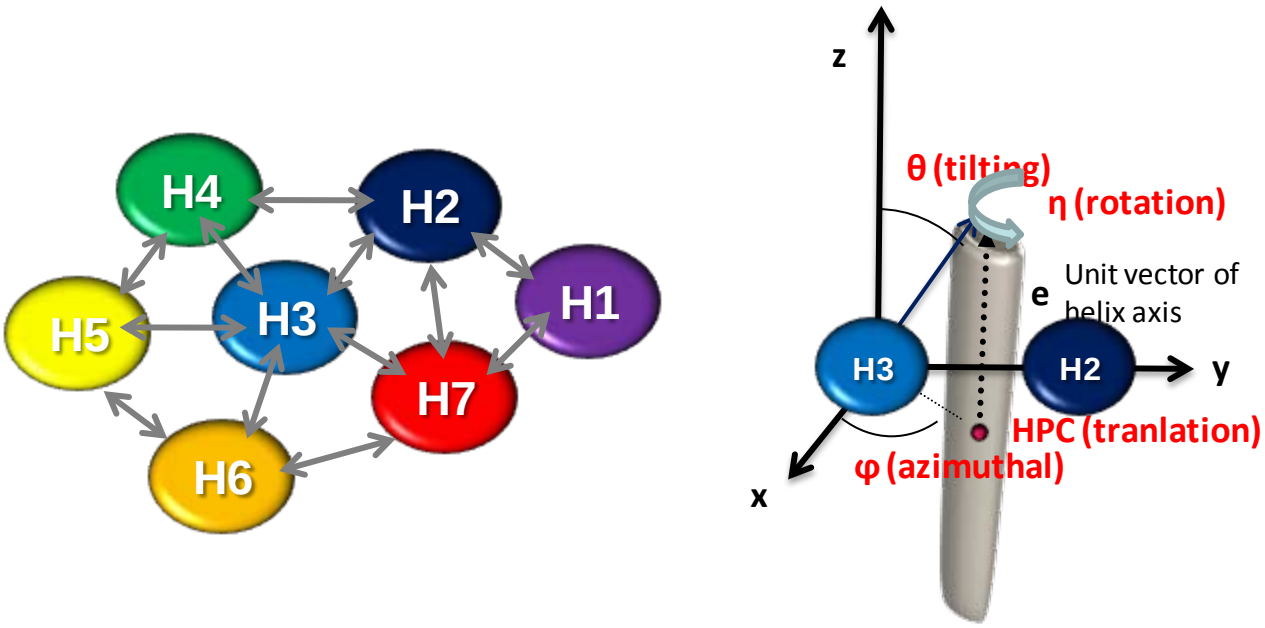

Figure S2. (Left) In Bihelix sampling, each helix pair is to simultaneously rotate through 360° in 30° increments, leading to $(12)^7$ = 35,000,000 configures. (Right) The tilt (θ) of each axis from the z-axis, the azimuthal orientation (φ) of this tilt; and the rotation (η) of the helix about the helical axis for SuperBihelix. The x-axis is defined along the axis from the center point of transmembranic helix (TMH) 3 to the center point of TMH2 in the midplane.

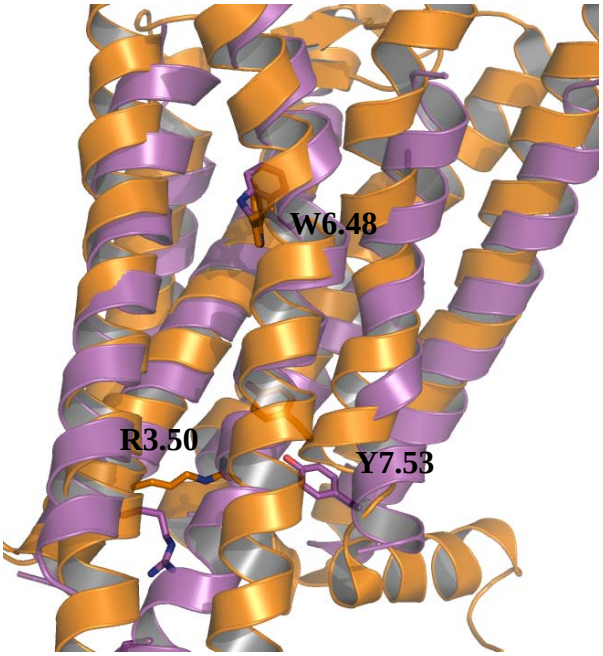

Figure S3. Predicted structure of agonist Cl-IB-MECA bound to adenosine A_3 receptor (15-apo-A_3) in purple and the opsin crystal structure (PDB ID: 3cap) in orange. This shows very similar configurations for the toggle residues: W6.48, Y7.53, and R3.50

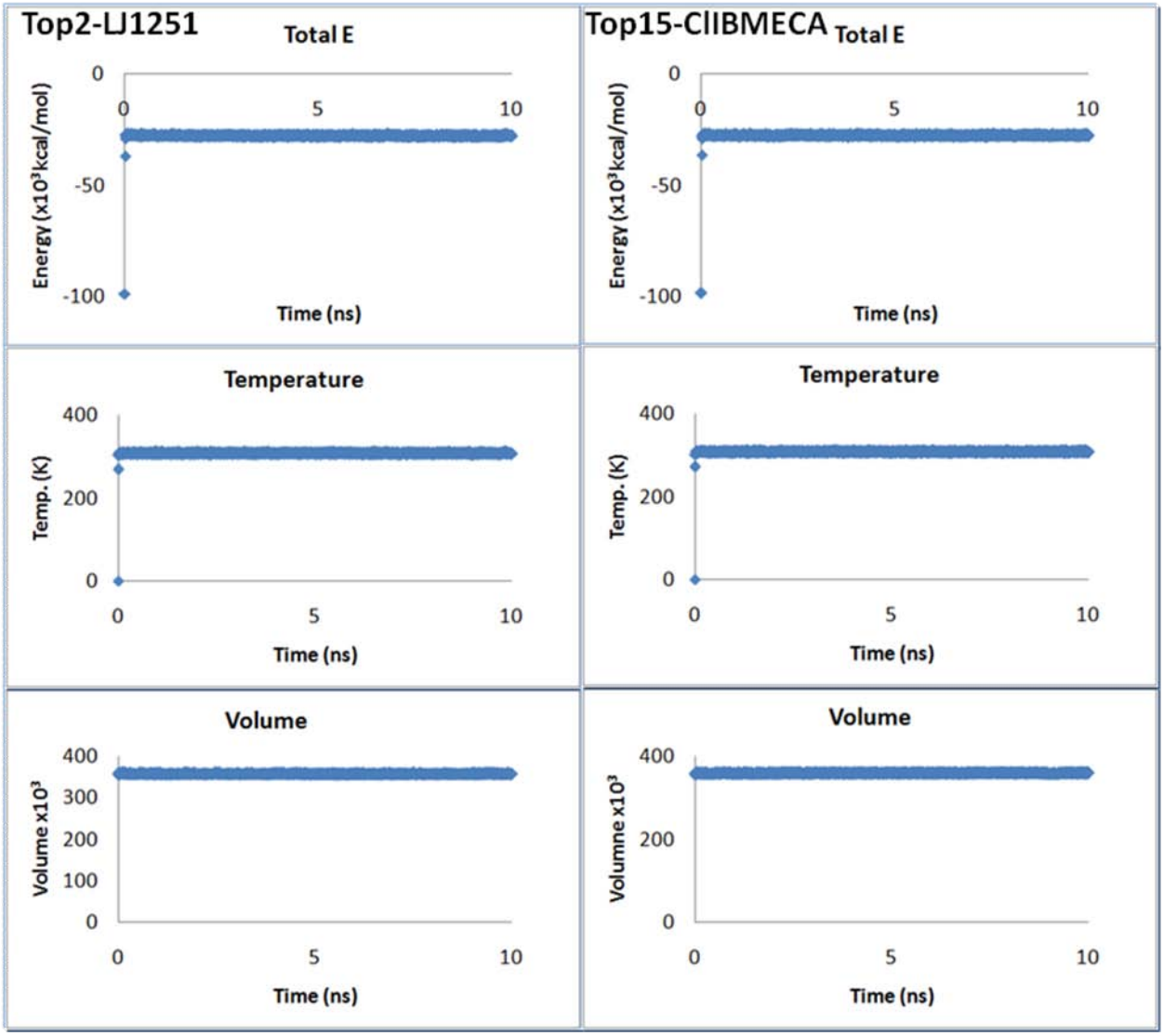

Figure S4. Total energy, temperature and volume of (Left) antagonist LJ1251 and (Right) agonist Cl-IB-MECA bound human adenosine A_3 receptor (hAA_3R) through 10ns dynamics.

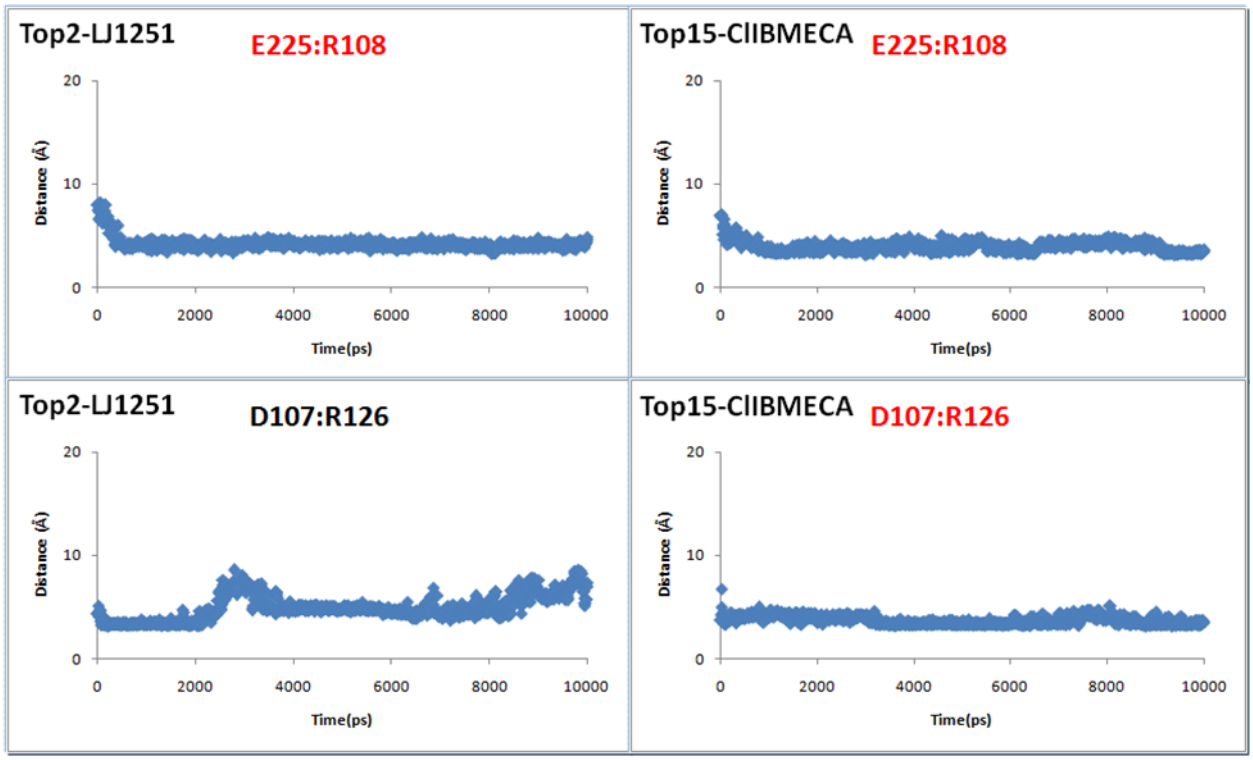

Figure S5. Important salt-bridges from (Top) R108$^{3.50}$ of the D(E)RY motif with E225$^{6.30}$ and from (Bottom) D107$^{3.49}$ with R126$^{4.41}$ of (Left) antagonist LJ1251 and (Right) agonist Cl-IB-MECA bound human adenosine A_3 receptor (hAA_3R) through 10ns dynamics.